



Review

Structural metamaterials with negative mechanical/thermomechanical indices: A review

João O. Cardoso, João Paulo Borges, Alexandre Velinho*

CENIMAT/i3N, Departamento de Ciência dos Materiais, Faculdade de Ciências e Tecnologia, Universidade Nova de Lisboa, Caparica, Portugal

ARTICLE INFO

Keywords:

Mechanical and thermomechanical metamaterials
Auxetic
Anepeptic
Negative Poisson's ratio
Negative thermal expansion
Negative linear compressibility

ABSTRACT

Structural metamaterials presenting negative values of one or more mechanical and thermomechanical indices – namely the Poisson's ratio, the linear compressibility, and the coefficient of thermal expansion – are the promising candidates to the applications in many fields, ranging from precision mechanics to biomedical devices or energy absorption. Although scattered mentions may be found in the literature since the late eighties of 20th century, the systematic research efforts concerning these materials became effective much later. The present work is to review the main scientific contributions to the topic in the last five years. This paper first deals with those metamaterials showing a single negative index, and then proceeds to analyze the much less frequent instances of coupled negative indices, with emphasis on the so-called anepeptic case, which exhibits an unusual thermomechanical response.

1. Introduction

Metamaterials are materials that are artificially engineered to gain properties and functionalities that are unattainable or at least unusual in naturally occurring or traditionally manufactured materials. Although metamaterials are more commonly associated with optics, electromagnetic, and electronic applications, recent developments concerning structural metamaterials noticeable for their mechanical/thermomechanical behavior deserve to be analyzed on their own merits.

The most studied properties in structural metamaterials are negative Poisson's ratio (NPR), negative thermal expansion coefficient (NTE), and negative linear compressibility (NLC). These revolve around essentially reversible deformations, which can be obtained by combining one or more base materials with a specific internal geometry [1]. The scheme in Fig. 1 summarizes the essence of each type of behavior.

Since they break apart from the known definite couplings to exist in conventional materials between different mechanical and thermal properties (e.g., denser materials are stronger than lighter ones, stiffer materials tend to have a higher thermal conductivity), the structural metamaterials offer the possibility to expand the regions in the material property space occupied by the materials for engineering applications; which explains why such metamaterials are currently attracting the researchers' attention.

Several good reviews concerning individual NPR [3,4] and NTE [5]

metamaterials have been published in the past. The present review, which is focused primarily on the literature made available from 2018 onwards, looks to the more recent developments concerning each individual behavior, comprising the less common property of NLC [6], and emphasizes research performed on combinations of the individual behaviors. Such combinations are pertinent as a current research topic due to the multiple potential applications [2].

In general, the structural metamaterials are built through prepetition of a unit cell with the desired properties to produce a lattice, or cellular structure.

2. Negative Poisson's ratio (NPR): auxetic metamaterials

According to Equation (1), the Poisson's ratio (ν) is defined as the ratio between two strains occurring along mutually perpendicular directions when stress is applied along one of those directions. In nature, this ratio for most materials has values between 0 (cork) and 0.5 (rubber).

$$\nu = -\frac{d\epsilon_{y^*}}{d\epsilon_x} \quad (1)$$

Materials are considered auxetic when the value of the Poisson's ratio is below zero. Auxeticity is present in some rare naturally occurring substances, an example being the rutherfordine mineral (UO_2CO_3), as

* Corresponding author.

E-mail address: ajv@fct.unl.pt (A. Velinho).

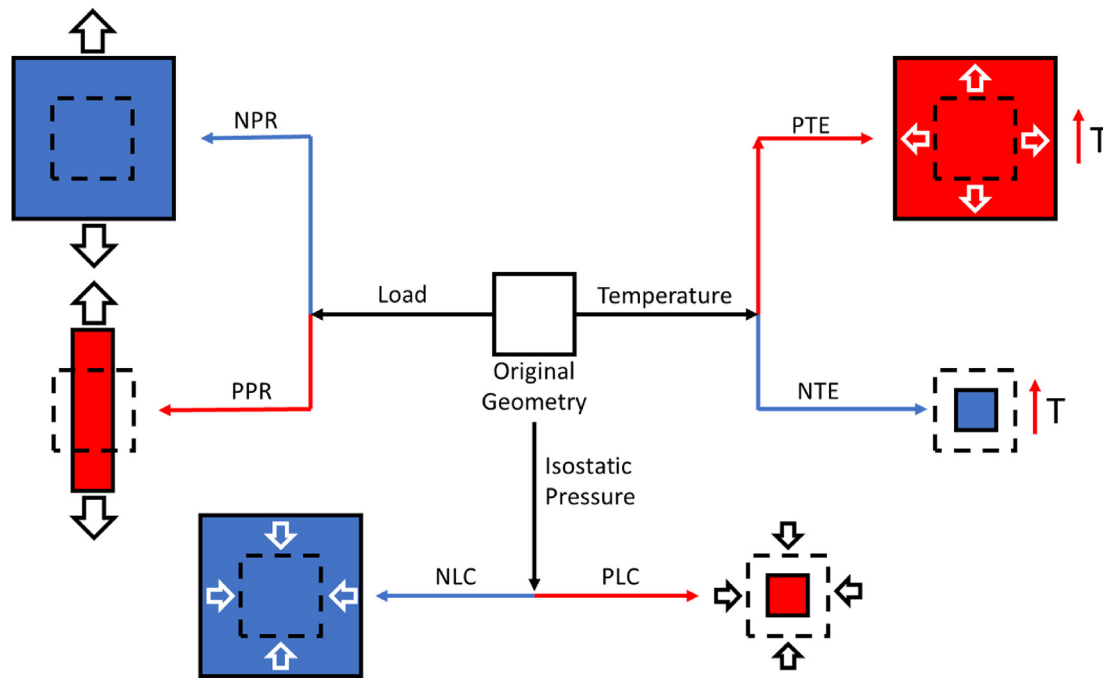


Fig. 1. Schematic representation of the different structural metamaterial behaviors. The Poisson's ratio controls the transverse deformation suffered by the material when subject to an effort applied along a specific direction; while materials with a positive Poisson's ratio (PPR) contract/expand laterally to the applied tensile/compressive stress, the reaction is switched for those with a negative Poisson's ratio (NPR). Similarly, if the material is subject to a compressive isostatic pressure, it will contract if it has a positive linear compressibility (PLC) but will otherwise expand with a negative linear compressibility (NLC). Finally, a positive thermal expansion (PTE) dictates that the material dilates/contracts when it is heated/cooled, while a negative thermal expansion (NTE) will determine otherwise. Of course, combined effects may be imagined. Adapted from [2].

discovered in 2018 by Colmenero [7]. Even before that, some natural materials like cow teat skin and live cat skin had been shown to exhibit such behavior [8]. Nevertheless, and for practical purposes, auxetic behavior is generally considered within the realm of engineered materials. Over the years, several structures conveying auxetic properties have been studied, even though some designs have gathered more attention than others.

NPR is a structural effect normally independent of the material it is made of. NPR structures respond to compressive stress by folding, rotating, or bending upon themselves, having the opposed behavior with an applied tensile stress.

Typically, auxetic structures, in both 2D and 3D, have been divided into five major categories based on their geometry: re-entrant, chiral, rotating, crumpled sheets, perforated sheets. From these, recent works dealing with crumpled auxetics seem to be non-existent. However, it should be noted that some structures studied don't fit neatly into a clear category, having therefore been classified simply as 'other'; examples of these are provided by Ren et al. [4] as nodule-fibril structures, missing rib structures, and others. Fig. 2 contains schematic representations of each auxetic category. These aid to understand that re-entrant structures derive their behavior from the fact that when a tensile (stretching) load is applied along the horizontal direction, the ribs are forced to move outward, and the structure expands along the vertical direction. For chiral auxetics, a load applied along a given direction induces the rotation of the rings, causing a similar deformation along the transverse direction. In the case of rotating auxetics, the behavior in cause results from the rotation of the square parts in response to an applied load. With crumpled sheet auxetics, the structure deforms out-of-plane in response to a tensile force, causing it to de-wrinkle and stretch across the transverse direction. Finally, perforated sheet auxetics deform in a similar fashion to rotating squares.

Each category of auxetic metamaterial presents characteristic traits which distinguish it from the remainder: re-entrant auxetics are easy to design and optimize thanks to the developments in beam theory, but are

easily prone to buckling failure; aside from requiring more flexible materials, chiral auxetics are able to maintain auxeticity under high compressive strains but their performance under tension is lacking; rotating auxetics are easy to design and optimize and the contact points can be reinforced by hinges, making for very robust structures, but the design options are more limited than for re-entrant structures; crumpled sheets are easy to manufacture but have a narrow range of Poisson's ratio and offer limited applicability; finally, perforated sheet auxetics, while also having a limited range of Poisson's ratio values, are very easy to manufacture using techniques that can easily be applied to hard materials.

Auxetic materials and structures can present superior shear resistance, indentation resistance, fracture resistance, synclastic behaviors, variable permeability and better energy absorption performance [4]. These characteristics allow for the construction of smart filters, sensors, medical devices and protective equipment [4]. Some potential applications may not yet be foreseen. As an example, X. Zheng et al. [9] used MATLAB to mathematically generate an auxetic structure which was subsequently fabricated using a polymeric material; the authors then proceeded to successfully nickel-plate it, thus improving its conductivity without sacrificing its auxeticity.

Two-dimensional mono-material auxetic structures are easy to produce; even the introduction of a second material within such structures places some added challenges but remains easily achievable. However, the passage to three-dimensional auxetic structures adds significant complexity, independently of the number of materials used, and narrows the array of manufacturing technologies almost exclusively to additive manufacturing (AM), making cost a paramount concern. Henceforth, AM technologies akin to 3D-printing shall be simply designated as 'printing' for shorthand. A comprehensive review of the relevance of AM techniques to produce auxetic structures is provided in Ref. [10]. Another challenge is the fact that most auxetic structures depend on the existence of porosity in its design, making them unsuitable for sustaining large loads or impacts [4].

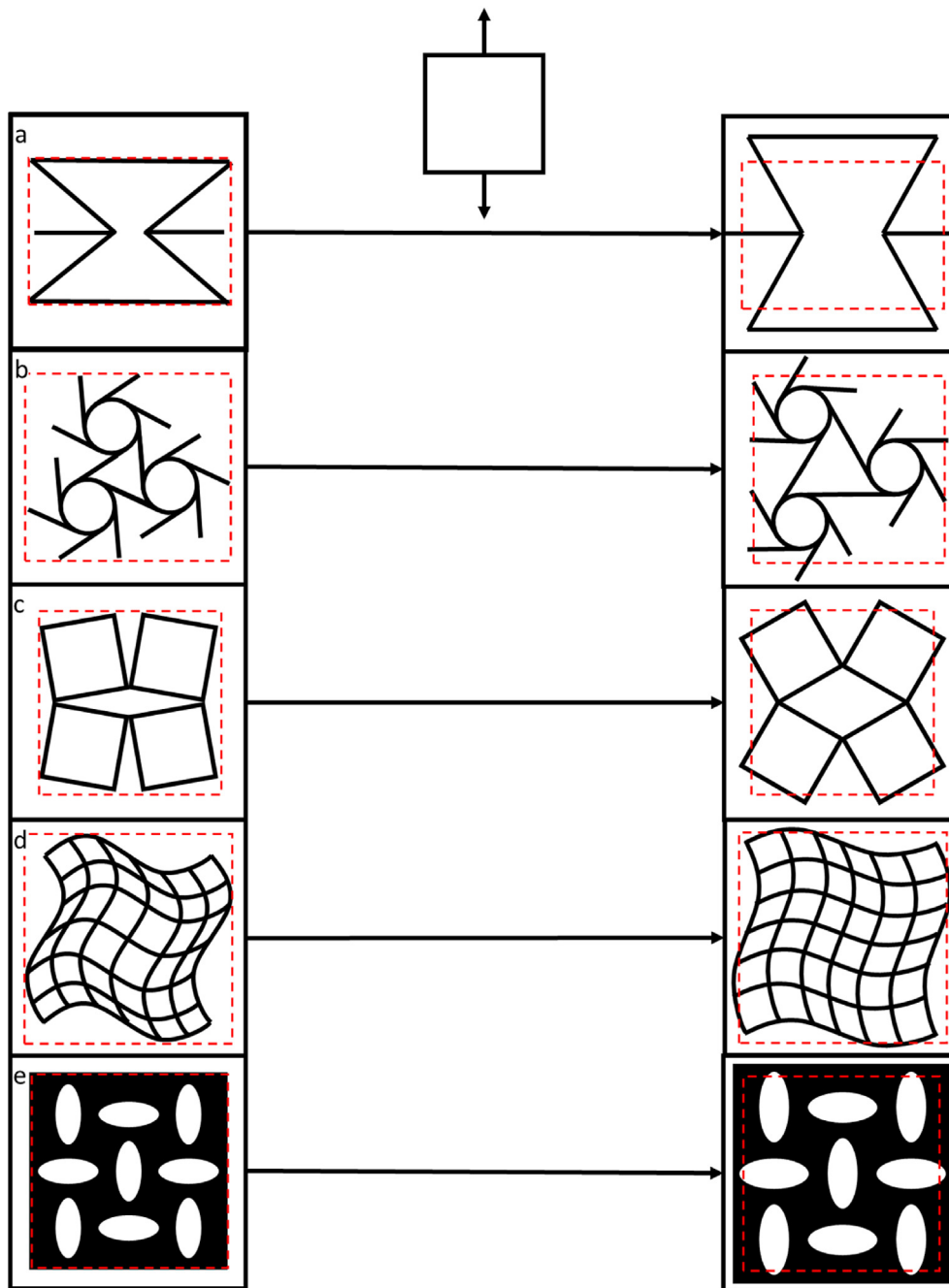


Fig. 2. Representative schematics of the typical geometries and deformations undergone under tension for each category of auxetic metamaterials: a) re-entrant; b) chiral; c) rotating; d) crumpled sheet; e) perforated sheet.

2.1. Re-entrant auxetic structures

Hamzehei et al. [11] developed three distinct 2D octagonal honeycomb auxetic structures printed in thermoplastic polyurethane (TPU) and mechanically tested them. Li et al. [12] altered the classical 2D re-entrant and double-arranged honeycomb (also known as double V and first described in Ref. [3]) structures by adding a middle strut, which improved the mechanical properties without sacrificing the NPR. Taherkhani et al. [13] used topology optimization to develop four different specimens of 2D re-entrant auxetic structures, which they printed using TPU. These authors then performed an in-depth study of the mechanical behavior of the structures, going past strains of 1.5 and achieving Poisson's ratio values down to - 2.44. B. Zheng et al. [14] studied a variant to the classical re-entrant honeycomb in which both

sides have the same angle (in contrast to having symmetrical angles) forming a parallelogram structure, for which the authors confronted calculated predictions and experimental data. Fabricating their structures with a UV-curable resin (Godart 8118), these authors then measured Poisson's ratios between - 0.210 and - 0.131, with Young's modulus ranging from 7.92 MPa to 45.29 MPa. They then used their validated model to simulate three kinds of 3D auxetic structures based on the newly developed 2D honeycomb, for which they predicted a minimum NPR of - 0.309.

Although studies concerning two-dimensional auxetics are still widely found, the focus has clearly shifted to three-dimensional structures. In 2018, Chen and Zheng [15] used modular digital light projection micro stereolithography technique coupled with *in situ* microfluidic systems for resin delivery to fabricate auxetic structures. Using several

known 3D re-entrant auxetic structures and two different basic monomers with dissimilar stiffness, they were able to tune the Poisson's ratio from -0.6 to 0. Their goal was to open a broad array of material-by-design applications, ranging from flexible armor, artificial muscles, to actuators and bio-mimetic materials.

V.H. Carneiro and H. Puga [16] designed and characterized auxetic structures based on re-entrant honeycombs that displayed a revolution axis. Within a specific density range between 0.28 and 0.35, the authors found that the axisymmetric structures showed gains in auxeticity (more pronounced negative values of the Poisson's ratio), together with a higher Specific Young's modulus.

Nasim and Etemadi [17] performed a comparison between Finite Element Analysis (FEA) model calculations and experimental findings for 3D auxetic re-entrant structures made from three different materials: 1100 aluminum alloy, 4340 Steel, and OFHC copper. The experimental data was found to be in good accordance with the predictions, an increase of the Poisson's ratio with the applied compressive strain being observed; the authors also tested three different re-entrant angles, which displayed very different starting results, but when the angles matched due to compression, the results became similar for all cases. There were not any significant differences regarding the nature of the tested materials. Huang et al. [18] used 3D-printed polymer-based semi-re-entrant honeycombs to obtain a PR of 0 for tissue engineering applications.

Geng et al. [19] developed a numerical model for predicting the mechanical properties of 3D re-entrant auxetic structures, such as stiffness, Poisson's ratio and strength. The authors then produced said structures in Al-Si10-Mg by selective laser melting and used *in situ* X-ray computed tomography to obtain the shape, position, and distribution of defects, after which such data was fed back into the FEA model. The authors concluded that there were large geometric errors between the samples and the numerical models, FEA simulations exhibiting higher load values than those obtained through experiments; the largest discrepancy found corresponding to a difference of 2000 N between the predicted 6000 N load compared to the 4000 N experimentally observed.

Some variations in the basic shape of the structures have been investigated. In this sense G. Gao et al. [20] developed an analytical model for the production of cylindrical structures with radial auxetic properties based on the double-arrowed honeycomb. After experimental validation, the authors used the simulations to design auxetic structures with tailored Young's modulus values.

Re-entrant auxetic structures lend themselves particularly well to the design of hierarchical structures. For this purpose, Qin et al. [21] developed a mathematical optimization model capable of designing lightweight metamaterials with specific Poisson's ratios, based upon which they proposed several new auxetic designs. Yang et al. [22] compiled the information on hierarchical metamaterials, presented a 3D hierarchical design strategy to systematically summarize the configuration characteristics, giving an excellent theoretical basis, and validating previous theoretical predictions with experimental data, namely nylon structures made by selective laser sintering.

Efforts to include designed variations in density and resulting properties throughout the structure have also been undertaken, combining functional gradients and auxeticity. Hedayati et al. [23] performed tension, compression, and shear tests on five different functionally graded auxetic meshes. Through the analysis of the strain distribution around the longitudinal and transversal directions, they were able to localize the maximum/minimum strain. The authors used the results to propose a new 'action-at-a-distance' concept, indicating it could be explored for remote-activated local actuators.

2.2. Chiral auxetic structures

Compared to the previous category, the availability of recent studies concerning the alternative types of auxetic structures is much smaller. Concerning chiral auxetics, Choi and Cho [24] ran several simulations of 2D structures with shape-memory polymers, but stopped short of a

working prototype, probably due to recognized unreliability of the materials used. Hu et al. [25] successfully printed 2D carbon fiber reinforced polylactic acid (PLA) to form auxetic chiral structures based on four geometries generated by a polynomial equation. The results showed that the auxeticity was accompanied by increased modulus, ultimate tensile strength, and energy absorption, coupled with decreased elongation at break. Auricchio et al. [26] printed tetra-chiral 2D honeycomb structures using acrylonitrile butadiene styrene (ABS), which were then submitted to uni-axial tension according to a force-control scheme. The results indicate a global Poisson's ratio close to -0.7 and a Young's Modulus of around 2 MPa. Attard et al. [27] developed an auxetic hierarchical 2D structure dubbed starchiral, which has the advantage that for some particular values of the design parameters the Poisson's ratio is insensitive to the dimensions of the structure, making it more tolerant to manufacturing defects. In particular, hexastarchiral structures have an inbuilt system that allows its Poisson's ratio to be varied.

Chirality has also been studied in the context of tridimensional structures. Ma and Peel [28] designed and printed a 3D spiral auxetic structure using an acrylic resin; the structure is capable of being woven into a shape-changing cloth, with applications in ballistic protection, easily cleaned filters or hosing. Wang et al. [29] obtained a good agreement between numerical and experimental results in 3D chiral strut-based auxetic structures to be used for energy absorption. The authors used selective laser sintering and white spherical polyamide 12 (PA12) powder to produce structures exhibiting increased normalized modulus, E^* , and normalized strength σ^* , for relative densities of around 0.1; the structures also present an energy efficiency parameter of around 80% and normalized specific energy absorption ($U_{M,n}$) as high as 0.2 for relative densities lower than 0.1.

It is also worth of notice the proposal from J. Gao et al. [30] for an isogeometric topology optimization method for efficiently designing auxetic composites, both re-entrant and chiral. The published work focuses heavily on the optimization and the algorithm used but is complemented with proposals for several 2D and 3D auxetic composite structures that could be produced.

2.3. Rotating auxetic structures

Two recent publications addressed rotating auxetic structures. Bacigalupo and Gambarotta [31] developed an analytical model to predict the properties of 2D chiral blocky structures. The work is extensive but does not consider the implications of adopting a particular material. Farrell et al. [32] went further along the experimental path, developing cylindrical auxetic structures inspired by deformed cell ligaments to be used as mechanical actuators. These authors designed their structures using FEA to optimize performance; the structures were subsequently printed using TPU. The study focused on measuring the structure's rotation in response to displacement, but no effort was made to evaluate the value of the Poisson's Ratio.

2.4. Perforated auxetic structures

A small number of recent advances have delved in the effect of H. Wang et al. [33] printed a 2D sheet with peanut-shaped holes using PLA, to study the effects the different parameters add in the Poisson's ratio, achieving values close to -1 for this parameter. Similarly, Liang and Crosby [34] developed an analytical model to predict the behavior of cellular flexible metamaterials, comparing the model's predictions with FEA simulations and experimental data, for which they used perforated sheets, which validated their design guideline for tailoring mechanical properties.

Box et al. [35] explored an efficient way to obtain hard auxetic metamaterials, through the perforation of metal or plastic plates with regular arrays of holes. The results obtained showed a change in the Poisson's ratio as the structures' elongation progresses.

2.5. Other geometries of auxetic structures

Several studies have been published concerning different geometries which don't fit into the pre-defined five categories. E.g. Favre et al. [36] investigated auxetic lattices with cubic symmetry using FEA as a tool to predict expected behavior as a function of the specific architecture parameters; their lattices' unit cells can be built up individually, offering a versatile solution for mechanical engineering; this procedure also offers the possibility to make architecturally graded materials, as well as to adjust the value of the Young's modulus within a suitable range while preserving a minimal density.

Similarly, Tozoni et al. [37] demonstrated that it is possible to build a family of auxetic and isotropic geometric structures from rhombic shapes with a large range of angles by following an analytical formula, making it possible for almost any structure to exhibit NPR properties.

Auxetic structures based on compliant mechanics were produced in 2D by Lima and Paulino [38], whereas Khare et al. [39] performed a similar work for the 3D case using a different methodology.

L. Wang et al. [40] in turn developed a double elliptical ring structure based on the latitude and longitude dimensions; this formed a 3D anisotropic auxetic structure. The authors calculated the structures' behavior using FEA, and then proceeded to achieve experimental validation of the results. The structures proposed in this work exhibit Poisson's ratio values below -10, with a theoretical limit of -18.3 in one direction.

A different approach has been developed in a series of publications by Z. Wang et al., culminating [41] in a systemized design of petal-based auxetics, validated experimentally. These have some interesting properties such as the Poisson's ratio changing linearly from around -0.9 to around -0.6 with the increase in engineering strain from -12% to almost 17%. These 2D structures also present out-of-plane buckling as part of their deformation method.

While most studies assume a linear elastic behavior of the constitutive material, Jeong and Yoo [42] used a non-linear beam theory to develop bowtie-shaped auxetic structures. This shape, which was chosen due to its simplicity, has been studied in the context of different engineering applications, and can be readily extended to 3D structures.

Instead of relying on a well-defined geometry, Reid et al. [43] designed isotropic auxetic metamaterials from random networks for applications ranging from robotics to impact mitigation. The authors laid out a framework for the design of tunable, highly auxetic isotropic materials; unlike most other cases, these results constitute one of the few continuous auxetic metamaterials.

Some attempts to confer auxeticity to foams have been undertaken. Based on numerical simulations, Liu et al. [44] analyzed the crashworthiness of cylindrical tubes filled with NPR foams, whereas Oh et al. [45] developed a method to produce graphene oxide-polyurethane foams for use in acoustic wave and shock energy dissipation.

Kolken et al. [46] studied the mechanical properties of metallic structures produced by selective laser melting in Ti-6Al-4V that combined auxetic and non-auxetic properties. The authors then used their results to produce hip replacements which they tested in a bone-mimicking setup.

Zong et al. [47] used a two-step analytical algorithm using FEA to design and optimize three distinct 3D auxetic structures. The simulation results were validated by experimental data, the authors using Selective Laser Sintering to print PA 2200 polyamide samples. The Poisson's ratio under compression was determined by digital image analysis.

3. Negative thermal expansion coefficient (NTE)

The linear thermal expansion coefficient (α_L) is a relevant parameter pertaining to the thermomechanical behavior of any material, correlating the strain observed along one direction with the change in temperature which causes it. This coefficient, which for any given material may be taken as constant within a specified temperature range, may thus be

defined in accordance with Equation (2), below:

$$\alpha_L = \frac{1}{L} \frac{dL}{dT} \quad (2)$$

Although in rigorous terms this should be evaluated independently for each direction in space, it can be assumed that for isotropic materials the coefficient remains the same irrespective of direction; for this reason, in such cases it is replaced by its volumetric equivalent, the coefficient of thermal expansion (α_V) (CTE), as defined by Equation (3):

$$\alpha_V = \frac{1}{V} \frac{dV}{dT} \quad (3)$$

Natural materials predominantly show positive values, but a few cases are known to present a negative thermal expansion (NTE), such as water between 0 and 4 °C and crystalline structures from the Zirconium tungstate (ZrW₂O₈) family [1].

According to Raminhos et al. [48] the NTE behavior results from the contributions of two constitutive materials with dissimilar properties: upon heating the structure, the stiffer material which simultaneously exhibits the smaller CTE "pushes" the other, more flexible but with higher CTE, material.

Unlike with auxetic materials, no effort is patent in the literature to separate different NTE structures into categories, despite observed similarities.

The study of NTE materials and structures is closely related to the need for materials capable of performing at a wide range of temperature without changing its volume, be it for cookware, laminates, or others. Using NTE materials also allows the design of composites whose CTE is tailored for its desired environment, such as in the case of dental fillings.

The main limitation of NTE materials is its dependence on the temperature range in which the effect is effective, which limits their use. Furthermore, the CTE may vary with temperature, causing additional engineering challenges.

Only a limited number of studies have been dedicated to the development of NTE metamaterials. K. Wei et al. [49] analyzed various 2D shapes for their CTE values, comparing them to their own design of a diamond shaped structure with tunable CTE within the range of -369.01 to 694.00 ppm K⁻¹. In turn, X. Guo et al. [50] designed a kirigami-inspired¹ hierarchical metamaterial with tunable CTE; these authors also performed a very extensive literature review, placing most publications into context. More recently, S. Savic-Šević et al. [51] achieved the first thermo-osmotic metamaterial with a large negative thermal expansion, developing a method capable of producing large-area NTE materials which may be applied to many different polymers. Finally, K. Wei et al. [52] obtained CTE values ranging from -77 to 258 ppm K⁻¹ for a 2D re-entrant structure made from Nylon and Poly(vinyl alcohol) (PVA); these authors followed an approach previously established by Raminhos et al. [48], consisting in selectively replacing structural elements of a re-entrant structure with a second material with adequate CTE and stiffness.

4. Negative linear compressibility (NLC)

Linear compressibility, described by Equation (4), relates a material's volume change under an applied hydrostatic stress; it is also known as the bulk modulus K (or B).

$$K = -V \frac{dP}{dV} \quad (4)$$

In 2018 J. Qu et al. [53] produced two three-dimensional poroelastic cubic metamaterials via 3D laser nano-lithography, a commercially available photoresist and mr-Dev 600 as the developer. The authors

¹ Origami is well-known the Japanese art of folding paper. Kirigami results from allowing the additional rule that paper cuts can be performed.

tested their structures' volume change with an applied pressure up to 3.8 bar; negative effective compressibility values of $k_{eff} = -4.7\%/bar$ and $k_{eff} = 5.0\%/bar$ were determined for the structures. The following year F. Colmenero et al. [54] discovered that uranyl squarate monohydrate $((UO_2)(C_4O_4) \cdot H_2O)$ naturally presented negative linear compressibility.

The NLC effect shows some similarity with the NTE, for it requires the simultaneous contribution of two constitutive materials with widely different reactions to applied pressure; coupled with a specific geometry, the balance resulting from the dissimilar deformation results on the overall NLC effect.

The development of NLC structures is interesting for the development of: pressure-sensing devices and actuators [55].

5. Metamaterials combining different negative indices

5.1. NPR & NTE: anepectic metamaterials

One important research development from recent years has been the search for different combinations of the effects shown above. Of these, the simultaneous occurrence of negative Poisson's ratio and coefficient of thermal expansion, for which some authors proposed the term 'Anepectic', derived from the Greek root " (Ἐπέκτασι), meaning expansion [48], seems to have gathered the largest interest. Anepectic metamaterials are considered potentially advantageous in fields as diverse as those of medicine, defense, sports, automobile, and aeronautics, even though they have only recently come to light and as such still warrant in-depth studies.

The anepectic behavior can be obtained by coupling two or more adequately chosen base materials with specific architectures. For some categories of known auxetic structures, namely re-entrant, chiral, and rotating, it is possible to pick which parts of the structure can be replaced with a second material of adequate stiffness and thermal expansion, to turn an auxetic structure into an anepectic one. This approach was previously applied for 2D meshes [48], and current work by the same authors aims at extending a similar result into the third dimension.

This is of course limited to very specific geometries and temperature ranges.

In terms of production, two-dimensional sheets can be relatively easy to fabricate. When trying to achieve three-dimensional structures, due to the multi-material requirement on top of the cellular structure, production is limited to AM, once again making cost the biggest concern.

One of the first mentions of the possibility to combine NPR with NTE corresponds to the 2017 work of C. Ng et al. [56], who have developed an analytical and numerical model to study the anisotropic and negative thermal expansion of bi-material re-entrant double V structures. Later, H. Yu et al. [57] designed planar chiral lattice structures and cylindrical shells capable of a wide range of tailorable equivalent CTEs, while H. Jopek and T. Stręk [58] studied the thermoauxetic behaviour of 2D composite structures. While all the previous works were limited in scope to the numerical simulation of the anepectic effect, Raminhos et al. [48] first reported the experimental development of 2D bi-material polymeric re-entrant meshes that presented both NPR and NTE.

In 2019 X. Li et al. [59] culminated a series of publications on the development of 2D anepectic metallic structures. Their original paper was a precursor to H. Yazdani Sarvestani et al. [60], which in 2021 expanded the initial concept and printed 3D bi-material polymeric structures with anepectic properties; however, these authors confronted difficulties while printing their samples, hence their work relies heavily on numerical simulations.

T. Lim [61] simulated the behavior of a composite microstructure with sign-switching Poisson's ratio depending on the stress direction. This structure also presents NTE or zero thermal expansion (ZTE) for certain design parameters. Later, the same author [62] designed and modeled a class of metamaterials made from alternating biomaterial and rigid crossbeams. Through judicious arrangements of the alternating

bi-material strips, these metamaterials can be made to exhibit (a) positive or negative properties regardless of the sign of the temperature change and, more interestingly, (b) positive or negative properties depending on that same sign.

N. Yang et al. [63] developed 3D anepectic kirigami structures using laser cut thick paper with a Young's modulus of about 2 GPa to which shape memory NiTi patches are glued according to specific geometries. These structures present a new building block for designing artificial materials with coded thermal expansion properties that support targeted isotropic and anisotropic deformations upon outside temperature changes. The paper shows that the thermal deformations can be tuned by changing angles, lengths, and fold types at the junction of the paper sheets; the paper also presents the possibility of increasing the structure's size without incurring in scaling-related difficulties.

M. Fu et al. [64] used beam theory to model three-dimensional auxetic materials with controllable thermal expansion. The strut-based structures developed, with predicted CTE as low as -45.6 ppm K^{-1} and -17.2 ppm K^{-1} for α_z and respectively and Poisson's ratio of -1 for ν_{xy} and 1.82 for ν_{xz} , were made from 7075 aluminum alloy, selectively replaced in specific sites with Invar or AISI 431 stainless steel.

X.-L. Peng and S. Bargmann [65,66] modeled a hybrid-honeycomb structure with enhanced stiffness, tunable auxeticity and negative thermal expansion coefficient, based upon the use of 6061 aluminum and Invar-36 alloys. The model predictions for the Poisson's ratio were in the -1 to 0 interval, with a CTE ranging between -15 and 0 , depending on the specific geometry.

5.2. Other combinations

Apart from anepectics, other combinations have been explored. Materials that present both NPR and NLC are exceptionally tailored for damping mechanisms, be it soundproofing, protective devices (car bumpers, seismic protection) or biomedical applications (stents, skin grafts, smart dressings and implants) [67]. In nature, this combined behavior was found by F. Colmenero [68] in silver oxalate ($Ag_2C_2O_4$), which shows a Poisson's ratio of -1.27 . It also presents anisotropic NLC for external pressures in the range -0.1 to -2.4 GPa directed along the [010] crystallographic direction and isotropic NLC for isostatic pressures in the range -0.51 to 13.4 GPa. The lowest value of the negative compressibility, $-831.9 \pm 10 \text{ TPa}^{-1}$, is found for an isostatic pressure of -0.16 GPa. Additionally, J. Grima-Cornish et al. [69] have discovered that boron arsenate (BAO_4) presented both NPR and NLC in the [001] plane.

In a similar fashion to how anepectic structures are conceived, a good research approach to try and develop this type of metamaterial is to start with an auxetic structure and change some of its materials with others presenting a dissimilar bulk modulus. This procedure generates a similar smart metamaterial whose activation is based on pressure instead of temperature. In this vein, E. Degabriele et al. [70] have modeled the compressibility properties of wine-rack-like-carbon allotropes and related poly(phenylacetylene) systems and found that these should theoretically possess NPR and NLC. Later J. Grima-Cornish et al. [71] have produced rotating square structures that exhibited highly negative values (-30) of Poisson's ratio together with negative compressibility, whereas K. Dudek et al. [67] have produced a multidirectional metallic auxetic structure with negative linear compressibility.

The alternate possibility of coupling a negative thermal expansion with a negative linear compressibility is comparatively under-developed, published work being limited to R. Cauchi et al. [72], which in 2020 have conceptualized several geometries allowing simultaneously for NTE and NLC. The concept is potentially interesting but has yet to be demonstrated experimentally.

Concerning the simultaneous coupling of the three effects (NPR, NTE and NLC), so far it has been found to be present in $Zn[Au(CN)_2]_2$, as discovered in 2017 by L. Wang et al. [73]. Such discovery is important, for it is a demonstration of the possibility of engineering a material with this behavior, but any advantages and limitations are still to be found,

pending theoretical and experimental work that may be performed in the future.

6. Conclusion

There are many studies concerning Poisson's ratio and its control, be it negative, near zero or sign switching; and most studies tend to go towards the goal of having a tailorable property to suit specific application needs. The next studied property is thermal expansion, and most studies are attempting to reach 0 or near 0 CTE values, as it seems to be the most desirable property. Linear compressibility is by far the least studied property, and the research on this subject is being still in the early exploratory stages.

Studying the combination of negative thermal or thermomechanical indices are less common overall, but the anepetic materials and structures dominate scientific literature, followed by the combination of NPR and NLC, which has many interesting applications; the studies on the combination of NTE and NLC are very rare and only one case has been found for the combination of all three properties.

When it comes to structures, authors are either fine-tuning 2D structures or testing 3D structures, the latter seeming to be the current trend. Many production challenges are being presented when producing 3D structures as most authors are using AM to that effect. Since in the more specific cases the intended behavior depends on the co-existence of two or more materials within the structure, the specific machinery is required for viable production, which is many times a strongly limiting factor to advances on the subject. Thus, the most current challenges lie in the production aspect, and more complicated structures are dependent on AM for its production. Finding alternative means for producing the desired structures, particularly for multi-material cases, would provide a major breakthrough.

The challenges inherent to effective fabrication of these metamaterials are also reflected by the fact that, even today, many publish studies are limited to modelling and simulation endeavors and lack experimental validation. Thus, the additional effort is warranted if structural metamaterials with negative indices are to fulfill their expected role in engineering applications.

Thus, the additional effort is warranted if structural metamaterials with negative indices are to fulfill their expected role in engineering applications. Such applications encompass the specific devices like prosthetics, smart filters, dampeners, sensors, and the actuators covering different fields such as: medical, automotive, aerospace, defense, precision mechanics, sports, textiles, and cookware. The differences in volume and rate of development of these fields, each contending with specific challenges regarding materials' behavior needs, are the main factor behind the amount of research dedicated to the different types of structural metamaterial.

Declaration of competing interest

The authors declare that they have no known competing financial interests or personal relationships that could have appeared to influence the work reported in this paper.

Acknowledgments

This work was funded by National Funds through FCT - Portuguese Foundation for Science and Technology, Reference UID/CTM/50025/2019.

João Cardoso acknowledges the funding by FCT – Fundação para a Ciência e Tecnologia under the research grant SFRH/BD/146227/2019.

References

- [1] T.-C. Lim, Springer, Singapore, 2020, <https://doi.org/10.1007/978-981-15-6446-8>. Singapore.

- [2] C. Huang, L. Chen, *Adv. Mater.* 28 (37) (2016) 8079–8096, <https://doi.org/10.1002/adma.201601363>.
- [3] K.K. Saxena, R. Das, E.P. Calius, *Adv. Eng. Mater.* 18 (11) (Nov. 2016) 1847–1870, <https://doi.org/10.1002/adem.201600053>.
- [4] X. Ren, R. Das, P. Tran, T.D. Ngo, Y.M. Xie, *Smart Mater. Struct.* 27 (2) (2018), 23001, <https://doi.org/10.1088/1361-665X/aaa61c>.
- [5] C. Lind, *Materials (Basel)*. 5 (6) (2012) 1125–1154, <https://doi.org/10.3390/ma5061125>.
- [6] R. Gatt, J.N. Grima, *Phys. Status solidi, Rapid Res. Lett.* 2 (5) (2008) 236–238, <https://doi.org/10.1002/pssr.200802101>.
- [7] F. Colmenero, *Appl. Sci.* 8 (no. 11) (2018), <https://doi.org/10.3390/app8112281>.
- [8] Y. Prawoto, *Comput. Mater. Sci.* 58 (2012) 140–153, <https://doi.org/10.1016/j.commatsci.2012.02.012>.
- [9] X. Zheng, X. Guo, I. Watanabe, *Mater. Des.*, 198 (2021), 109313, <https://doi.org/10.1016/j.matdes.2020.109313>.
- [10] A. Joseph, V. Mahesh, D. Harursampath, *Adv. Manuf.*, 2 (2021), <https://doi.org/10.1007/s40436-021-00357-y>.
- [11] R. Hamzehei, J. Kadkhodapour, A.P. Anaraki, S. Rezaei, S. Dariushi, A.M. Rezaoust, *Int. J. Mech. Sci.* 145 (2018) 96–105, <https://doi.org/10.1016/j.ijmecsci.2018.06.040>, no. June.
- [12] X. Li, Q. Wang, Z. Yang, Z. Lu, *Extrem. Mech. Lett.* 27 (2019) 59–65, <https://doi.org/10.1016/j.eml.2019.01.002>.
- [13] B. Taherkhani, A.P. Anaraki, J. Kadkhodapour, S. Rezaei, H. Tu, J. *Elastomers Plast.* (2020), <https://doi.org/10.1177/0095244320938411>.
- [14] B. Bin Zheng, F.M. Liu, L.L. Hu, M.H. Fu, Y. Chen, *Int. J. Mech. Sci.* 161–162 (2019), 105073, <https://doi.org/10.1016/j.ijmecsci.2019.105073> no. August.
- [15] D. Chen, X. Zheng, *Sci. Rep.* 8 (1) (2018) 1–8, <https://doi.org/10.1038/s41598-018-26980-7>.
- [16] V.H. Carneiro, H. Puga, *Compos. Struct.*, 204 (2018) 438–444, <https://doi.org/10.1016/j.compstruct.2018.07.116>, no. July.
- [17] M. Safikhani Nasim, E. Etemadi, *Int. J. Mech. Sci.*, 136 (2018) 475–481, <https://doi.org/10.1016/j.ijmecsci.2018.01.002>, no. January.
- [18] J. Huang, W. Liu, A. Tang, *Mater. Sci. Eng. B solid-state mater. Adv. Technol.* 236–237 (2018) 95–103, <https://doi.org/10.1016/j.mseb.2018.11.005>, no. January.
- [19] L. Geng, W. Wu, L. Sun, D. Fang, *Int. J. Mech. Sci.* 157–158 (2019) 231–242, <https://doi.org/10.1016/j.ijmecsci.2019.04.054>, no. February.
- [20] Q. Gao, W.H. Liao, L. Wang, *Int. J. Mech. Sci.* 173 (2020), 105400, <https://doi.org/10.1016/j.ijmecsci.2019.105400> no. January.
- [21] H. Qin, D. Yang, C. Ren, *Materials (Basel)*. 11 (9) (2018), <https://doi.org/10.3390/ma11091574>.
- [22] H. Yang, B. Wang, L. Ma, *Compos. Struct.* 214 (2019) 359–378, <https://doi.org/10.1016/j.compstruct.2019.01.076>, no. February.
- [23] R. Hedayati, M.J. Mirzaali, L. Vergani, A.A. Zadpoor, *APL Mater.*, 6 (3) (2018), <https://doi.org/10.1063/1.5019782>.
- [24] M.J. Choi, S. Cho, *Struct. Multidiscip. Optim* 58 (5) (2018) 1861–1883, <https://doi.org/10.1007/s00158-018-2088-y>.
- [25] C. Hu, J. Dong, J. Luo, Q.H. Qin, G. Sun, *Compos. Part B Eng.*, 201 (2020), 108400, <https://doi.org/10.1016/j.compositesb.2020.108400> no. August.
- [26] F. Auricchio, A. Bacigalupo, L. Gambarotta, M. Lepidi, S. Morganti, F. Vadalà, *Mater. Des.* 179 (2019), <https://doi.org/10.1016/j.matdes.2019.107883>.
- [27] D. Attard, P.S. Farrugia, R. Gatt, J.N. Grima, *Int. J. Mech. Sci.* 179 (2020), <https://doi.org/10.1016/j.ijmecsci.2020.105631> no. November 2019.
- [28] Q. Ma, L.D. Peel, *Compos. Struct.* 192 (2018) 310–316, <https://doi.org/10.1016/j.compstruct.2018.02.091>, no. November 2017.
- [29] Q. Wang, Z. Li, Y. Zhang, S. Cui, Z. Yang, Z. Lu, *Composites Part B Eng.* 202 (2020), 108379, <https://doi.org/10.1016/j.compositesb.2020.108379> no. April.
- [30] J. Gao, M. Xiao, L. Gao, J. Yan, W. Yan, *Comput. Methods Appl. Mech. Eng.* 362 (2020), 112876, <https://doi.org/10.1016/j.cma.2020.112876>.
- [31] A. Bacigalupo, L. Gambarotta, *Extrem. Mech. Lett.* 39 (2020), 100769, <https://doi.org/10.1016/j.eml.2020.100769>.
- [32] D.T. Farrell, C. McGinn, G.J. Bennett, *Compos. Struct.* 238 (2020), 111901, <https://doi.org/10.1016/j.compstruct.2020.111901> no. August 2019.
- [33] H. Wang, Y. Zhang, W. Lin, Q.H. Qin, *Comput. Mater. Sci.* 171 (2020), 109232, <https://doi.org/10.1016/j.commatsci.2019.109232> no. August 2019.
- [34] X. Liang, A.J. Crosby, *Extrem. Mech. Lett.* 35 (2020), 100637, <https://doi.org/10.1016/j.eml.2020.100637>.
- [35] F. Box, C.G. Johnson, D. Pihler-Puzović, *Extrem. Mech. Lett.* 40 (2020), 100980, <https://doi.org/10.1016/j.eml.2020.100980>.
- [36] J. Favre, P. Lohmuller, B. Piotrowski, S. Kenzari, P. Laheurte, F. Meraghi, *Addit. Manuf.* 21 (2018) 359–368, <https://doi.org/10.1016/j.addma.2018.02.020>, no. January.
- [37] D.C. Tozoni, J. Dumas, Z. Jiang, J. Panetta, D. Panozzo, D. Zorin, *ACM Trans. Graph.* 39 (4) (2020), <https://doi.org/10.1145/3386569.3392451>.
- [38] C.R. de Lima, G.H. Paulino, *Adv. Eng. Softw.* 129 (2019) 69–80, <https://doi.org/10.1016/j.advengsoft.2018.12.002>, no. May 2018.
- [39] E. Khare, S. Temple, I. Tomov, F. Zhang, S.K. Smoukov, *Front. Mater.* 5 (2018) 1–11, <https://doi.org/10.3389/fmats.2018.00045>, no. August.
- [40] L. Wang, et al., *Extrem. Mech. Lett.* 42 (2021), 101142, <https://doi.org/10.1016/j.eml.2020.101142>.
- [41] Z.P. Wang, L.H. Poh, Y. Zhu, J. Dirrenberger, S. Forest, *Mater. Des.* 170 (2019), 107669, <https://doi.org/10.1016/j.matdes.2019.107669>.
- [42] S. Jeong, H.H. Yoo, *Compos. Struct.* 224 (2019), 111020, <https://doi.org/10.1016/j.compstruct.2019.111020> no. March.
- [43] D.R. Reid, N. Pashine, A.S. Bowen, S.R. Nagel, J.J. De Pablo, *Soft Matter* 15 (40) (2019) 8084–8091, <https://doi.org/10.1039/c9sm01241a>.

- [44] W. Liu, J. Huang, X. Deng, Z. Lin, L. Zhang, *Thin-Walled Struct.* 131 (2018) 297–308, <https://doi.org/10.1016/j.tws.2018.07.004>, no. May.
- [45] J.H. Oh, J.S. Kim, V.H. Nguyen, I.K. Oh, *Compos. Part B Eng.* 186 (2020), 107817, <https://doi.org/10.1016/j.compositesb.2020.107817> no. September 2019.
- [46] H.M.A. Kolkken, S. Janbaz, S.M.A. Leeftang, K. Lietaert, H.H. Weinans, A.A. Zadpoor, *Mater. Horizons* 5 (1) (2018) 28–35, <https://doi.org/10.1039/c7mh00699c>.
- [47] H. Zong, H. Zhang, Y. Wang, M.Y. Wang, J.Y.H. Fuh, *Mater. Des.* 159 (2018) 90–102, <https://doi.org/10.1016/j.matdes.2018.08.032>.
- [48] J.S. Raminhos, J.P. Borges, A.J. da C. Velhinho, *Smart Mater. Struct.* (2019), <https://doi.org/10.1088/1361-665x/ab034b>.
- [49] K. Wei, X. Xiao, J. Chen, Y. Wu, M. Li, Z. Wang, *Mater. Des.* 198 (2021), 109343, <https://doi.org/10.1016/j.matdes.2020.109343>.
- [50] X. Guo, et al., *Adv. Mater.* 33 (3) (2021) 1–12, <https://doi.org/10.1002/adma.202004919>.
- [51] S. Savić-Šević, et al., *J. Mater. Chem. C* (2021), <https://doi.org/10.1039/d1tc01028j>.
- [52] K. Wei, X. Xiao, W. Xu, Z. Han, Y. Wu, Z. Wang, *Virtual Phys. Prototyp.* 16 (S1) (2021) S53–S65, <https://doi.org/10.1080/17452759.2021.1917295>.
- [53] J. Qu, M. Kadic, M. Wegener, *Extrem. Mech. Lett.*, 22 (2018) 165–171, <https://doi.org/10.1016/j.eml.2018.06.007>.
- [54] F. Colmenero, J. Cobos, V. Timón, *J. Phys. Condens. Matter* 31 (17) (2019), <https://doi.org/10.1088/1361-648X/ab0312>.
- [55] A.B. Cairns, A.L. Goodwin, *Phys. Chem. Chem. Phys.* 17 (32) (2015) 20449–20465, <https://doi.org/10.1039/c5cp00442j>.
- [56] C.K. Ng, K.K. Saxena, R. Das, E.I. Saavedra Flores, *J. Mater. Sci.* 52 (2) (2017) 899–912, <https://doi.org/10.1007/s10853-016-0385-7>.
- [57] H. Yu, W. Wu, J. Zhang, J. Chen, H. Liao, D. Fang, *Compos. Struct.* 210 (2019) 327–338, <https://doi.org/10.1016/j.compstruct.2018.11.043>. November 2018.
- [58] H. Jopek, T. Stręk, *Materials (Basel)*. 11 (2) (2018), <https://doi.org/10.3390/ma11020294>.
- [59] X. Li, L. Gao, W. Zhou, Y. Wang, Y. Lu, *Extrem. Mech. Lett.* 30 (2019), 100498, <https://doi.org/10.1016/j.eml.2019.100498>.
- [60] H. Yazdani Sarvestani, A.H. Akbarzadeh, D. Therriault, M. Lévesque, *Compos. Struct.* 263 (May 2021), 113705, <https://doi.org/10.1016/j.compstruct.2021.113705>. February.
- [61] T.C. Lim, *Compos. Struct.* 209 (2019) 34–44, <https://doi.org/10.1016/j.compstruct.2018.10.074>. August 2018.
- [62] T.C. Lim, *Compos. Struct.* 226 (2019), 111256, <https://doi.org/10.1016/j.compstruct.2019.111256>. May.
- [63] N. Yang, M. Zhang, R. Zhu, *Extrem. Mech. Lett.* 40 (2020), 100912, <https://doi.org/10.1016/j.eml.2020.100912>.
- [64] M. Fu, J. Huang, B. Zheng, Y. Chen, C. Huang, *Smart Mater. Struct.* 29 (8) (2020), <https://doi.org/10.1088/1361-665X/ab9dda>.
- [65] X.L. Peng, S. Bargmann, *Extrem. Mech. Lett.* 43 (2021), 101201, <https://doi.org/10.1016/j.eml.2021.101201>.
- [66] X.L. Peng, S. Bargmann, *Int. J. Mech. Sci.* 190 (August 2020) (2021), 106021, <https://doi.org/10.1016/j.ijmecsci.2020.106021>.
- [67] K.K. Dudek, D. Attard, R. Gatt, J.N. Grima-Cornish, J.N. Grima, *Materials (Basel)*. 13 (9) (May 2020) 2193, <https://doi.org/10.3390/ma13092193>.
- [68] F. Colmenero, *Adv. Theory Simulations* 2 (6) (2019) 1–9, <https://doi.org/10.1002/adts.201900040>.
- [69] J.N. Grima-Cornish, L. Vella-Žarb, J.N. Grima, *Ann. Phys.* 532 (5) (2020) 1–6, <https://doi.org/10.1002/andp.201900550>.
- [70] E.P. Degabriele, et al., *Phys. Status Solidi Basic Res.* 256 (1) (2019) 1–10, <https://doi.org/10.1002/pssb.201800572>.
- [71] J.N. Grima-Cornish, J.N. Grima, D. Attard, *Materials (Basel)* 13 (1) (2020) 79, <https://doi.org/10.3390/ma13010079>.
- [72] R. Cauchi, D. Attard, J.N. Grima-Cornish, J.N. Grima, *Phys. Status Solidi Basic Res.* 1900633 (2020) 1–17, <https://doi.org/10.1002/pssb.201900633>.
- [73] L. Wang, H. Luo, S. Deng, Y. Sun, C. Wang, *Inorg. Chem* 56 (24) (2017) 15101–15109, <https://doi.org/10.1021/acs.inorgchem.7b02416>.